NPS-57Ph74111

NAVAL POSTGRADUATE SCHOOL

Monterey, California

SPINNING MISSILE MAGNUS FORCE MEASUREMENTS

H. L. Power

November 1974

Technical Report for Period January 1974-November 1974

Approved for public release; distribution unlimited

pared for:
ef of Naval Research
ington, Virginia 22217

NAVAL POSTGRADUATE SCHOOL

Monterey, California

Rear Admiral I. W. Linder
Superintendent

Jack R. Borsting
Provost

The work reported herein was supported by the Foundation Research Program at the Naval Postgraduate School.

This report was prepared by:

UNCLASSIFIED

SECURITY CLASSIFICATION OF THIS PAGE *(When Date Entered)*

REPORT DOCUMENTATION PAGE		READ INSTRUCTIONS BEFORE COMPLETING FORM
1. REPORT NUMBER NPS-57Ph74111	2. GOVT ACCESSION NO.	3. RECIPIENT'S CATALOG NUMBER
4. TITLE *(and Subtitle)* SPINNING MISSILE MAGNUS FORCE MEASUREMENTS		5. TYPE OF REPORT & PERIOD COVERED Technical Report 1 Jan 1974 - 1 Nov 1974
		6. PERFORMING ORG. REPORT NUMBER
7. AUTHOR(s) H. L. Power		8. CONTRACT OR GRANT NUMBER(s)
9. PERFORMING ORGANIZATION NAME AND ADDRESS Naval Postgraduate School Monterey, California 93940		10. PROGRAM ELEMENT, PROJECT, TASK AREA & WORK UNIT NUMBERS 61152N, RR 000-01-10, PO 4-0001
11. CONTROLLING OFFICE NAME AND ADDRESS Naval Postgraduate School Monterey, California 93940		12. REPORT DATE November 1, 1974
		13. NUMBER OF PAGES 30
14. MONITORING AGENCY NAME & ADDRESS *(if different from Controlling Office)* Chief of Naval Research Arlington, Virginia 22217		15. SECURITY CLASS. *(of this report)* Unclassified
		15a. DECLASSIFICATION/DOWNGRADING SCHEDULE
16. DISTRIBUTION STATEMENT *(of this Report)* Approved for public release; distribution unlimited		
17. DISTRIBUTION STATEMENT *(of the abstract entered in Block 20, if different from Report)*		
18. SUPPLEMENTARY NOTES		
19. KEY WORDS *(Continue on reverse side if necessary and identify by block number)* Spinning Missile Magnus Force		
20. ABSTRACT *(Continue on reverse side if necessary and identify by block number)* Wind tunnel data to determine Magnus force and center of pressure location on a spinning missile at angle of attack was correlated to a crossflow analogy theory with good results.		

DD FORM 1 JAN 73 1473 (Page 1)

EDITION OF 1 NOV 65 IS OBSOLETE

S/N 0102-014-6601

UNCLASSIFIED

SECURITY CLASSIFICATION OF THIS PAGE *(When Data Entered)*

TABLE OF CONTENTS

Section		Page
I.	Acknowledgement	2
II.	Nomenclature	3
III.	Introduction	4
IV.	Magnus Force Predictions	5
V.	Experimental Magnus Measurements	11
VI.	Conclusions	24
VII.	Cited References	26
VIII.	List of Figures	27
IX.	Computer Program	28

I. ACKNOWLEDGEMENT

The author wishes to thank Professor J. D. Iverson, Iowa State University, for his generous loan of portions of the test model, and to the Department of Aeronautics technicians for their help in constructing the test model balance and associated electronics. The work was supported, in part, by funds from the Foundation Research Program at the Naval Postgraduate School.

II. NOMENCLATURE

C_Y	Magnus force coefficient based upon freestream velocity and side area
C_{Yp}	$\partial C_Y / \partial \bar{p}$
C_1, C_2	Sideforce correlation constants for small and large α respectively
D	Cylinder diameter
L	Cylinder length
M_∞	Freestream Mach number
$\bar{p}$	Dimensionless spin rate (V/U)
q	Freestream dynamic pressure
r_o	Cylinder radius
R_L	Reynolds number based on cylinder length
R_c	Crossflow Reynolds number based on crossflow velocity and diameter
U	Freestream velocity of spinning missile
U_∞	Freestream velocity of rotating cylinder at 90° α
V	Cylinder surface speed
x	Longitudinal distance from nose
Y	Sideforce
α	Angle of attack
ω	Spin angular velocity
ν	Kinematic viscosity

III. INTRODUCTION

The production of sideforce (Magnus effect) on spinning bodies at angle of attack has been of interest to aerodynamicists since the 1800's when G. Magnus published the first experimental results of the drift of musket shot due to spin. Since that time, it has been recognized that accurate prediction of Magnus forces was necessary to calculate the trajectory and stability of spinning shell and missiles. In spite of all the time and effort expended since the 1800's, theoretical predictions of Magnus force production are extremely crude. Although the basic mechanism for Magnus force production is recognized, the mathematical model required for solutions considering bodies with even reasonably simple shapes is too complex and time consuming even for today's sophisticated fluid mechanics calculation methods. The engineer is forced, then, to use the very simple phenomenological models developed to date in conjunction with experimental correlations to make estimates of the Magnus effect on spinning missiles. This report gives the details of such a study.

IV. MAGNUS FORCE PREDICTIONS

It is generally agreed that Magnus force production is due entirely to viscous effects. An asymmetrical boundary layer is produced on the missile surface by the combined effects of spin and angle of attack. At very low angles of attack the boundary layer is attached over most of the missile length so that sideforce predictions may be based upon displacement thickness and shearing stress calculations. At larger angles of attack the asymmetrical boundary layer separates causing a shedding of vorticity into the outer inviscid flow. The shed vorticity induces an equal but opposite circulation in the outer flow producing an additional circulation sideforce contribution. The modeling of such a three-dimensional boundary layer separation problem is beyond the capabilities of present day theoretical techniques even for the relatively simple case of an incompressible, laminar flow over a rotating body of revolution with a cylindrical afterbody. Theoretical predictions of the effect of compressibility and a turbulent boundary layer on Magnus force must necessarily be even more crude.

At low angles of attack and small nondimensional spin rates the most realistic incompressible, laminar flow theory to date is that of Kelly.[1] Kelly considered the outer flow of an open ended rotating circular cylinder at an angle of attack. A perturbation solution of the boundary layer equations was used to calculate displacement thickness and shearing stress contributions to the Magnus force. The effects of a forebody and shed boundary layer vorticity were not considered. At very low angles of attack and for a high fineness ratio body this linear theory yeilds a reasonable estimate of the Magnus force.

For larger angles of attack (but still small) Power and Iverson[2,3] made an estimate of the Magnus force contribution due to boundary layer shed vorticity. This theory will be outlined in more detail because the

sideforce experimental data correlation used in this report originated from this work.

Following Kelly's lead, the incompressible, laminar flow about an open-ended circular cylinder at angle of attack shown in figure V-1 was considered. It was assumed that the effect of shed vorticity could be modeled by using a crossflow analogy. The circulation induced into the outer flow was approximated by assuming that the crossflow along the longitudinal cylinder axis was similar to the unsteady solution for the flow over an impulsively rotated cylinder placed perpendicular to the freestream as shown in Figure V-2. Values of the time dependent lift coefficient for the impulsively rotated cylinder where estimated from the results of Thoman and Szewczyk.[4] It was found that this data correlates very well by the relationship:

$$C_{\ell}(t) = f\left(\frac{V}{U_{\infty}}\right)\left\{1 - e^{-\frac{U_{\infty}t}{D}/\sqrt{\frac{U_{\infty}D}{\nu}}}\right\} \qquad \text{(IV.1)}$$

where U_{∞} is the freestream velocity, D is the cylinder diameter, and V is the cylinder surface speed. The crossflow analogy assumes that:

$$U_{\infty} = U \sin \alpha$$

$$t = \frac{\alpha}{U \cos \alpha} \qquad \text{(IV.2)}$$

$$\frac{V}{U_{\infty}} = \frac{\bar{p}}{\sin \alpha}$$

Using the additional assumption that $f(\frac{V}{U_{\infty}})$ can be approximated by a linear function the local Magnus sideforce coefficient based on diameter and crossflow velocity is given by:

$$C_Y(x) = C_o\left(\frac{\bar{p}}{\sin \alpha}\right)\left\{1 - e^{\frac{-x}{\bar{d}} \tan \alpha / R_d^{\frac{1}{4}} \sin^{\frac{1}{2}}\alpha}\right\} \qquad \text{(IV.3)}$$

where C_o is a constant.

For small angles of attack equation (V.3) leads to an equivalent local circulation strength given by

$$k(x) = \frac{\Gamma(x)}{\Gamma_o} = C_1 R_c^{3/4}\left(\frac{\nu x}{r_o^2 U}\right) \qquad \text{(IV.4)}$$

where C_1 is a constant, R_c is the crossflow Reynolds number based on crossflow velocity and the cylinder diameter, and Γ_o is the surface circulation strength. The total Magnus sideforce was calculated by integrating the local circulation contributions over the length and adding the contribution due to displacement thickness and shearing stress asymmetry. The result for small α and nondimensional spin rate $\bar{p} = V/U$ is:

$$C_Y = k_1\alpha + k_2\alpha^{7/4} \qquad \text{(IV.5)}$$

where:

$$k_1 = \frac{\pi}{4}\left(\frac{L}{D}\right)\frac{\bar{p}}{R_L^{\frac{1}{2}}}\left\{60.97 - 357.37\left(\frac{L}{D}\right)\frac{1}{R_L^{\frac{1}{2}}} - 227.01\left(\frac{L}{D}\right)^2\frac{1}{R_L}\right\}$$

$$k_2 = \frac{\pi}{4}\left(\frac{L}{D}\right)^{5/4}\frac{\bar{p}}{R_L^{\frac{1}{4}}}\,C_1$$

and the Magnus coefficient is based on the side area LD.

Equation (V.5) predicts that for a given missile configuration, spin rate, speed, and altitude, the sideforce coefficient is nonlinear with α. The constant C_1 can be evaluated by considering experimental data for cases which are consistent with the assumptions required for crossflow analogy application. It would also be expected that C_1 might be a function of Mach number because of compressibility effects. Because of the

low crossflow velocities at low angles of attack, crossflow Reynolds numbers are low enough for the laminar assumption to be valid even at high forward speeds.

Equation's (V.5) nonlinearity suggests that the dominant Magnus force production mechanism is shed vorticity at higher angle of attack. If this assumption is made, a much simpler correlation suggested by Iverson[5] can be developed. Returning to the result of equation V.3, an integration of the circulation produced local sideforce results in a Magnus force given by:

$$C_Y = C_o \bar{p} \sin \alpha \left\{ 1 + \frac{1}{Lu}(e^{-uL} - 1) \right\}$$

where

$$u \equiv \frac{\tan \alpha}{D} / R_d^{\frac{1}{4}} \sin^{\frac{1}{4}} \alpha$$

By expanding the exponential we find that

$$C_Y = \frac{C_o}{2} \bar{p} \left(\frac{L}{D}\right)^{5/4} \tan\alpha \sin^{3/4}\alpha \left(\frac{1}{R_L^{\frac{1}{4}}}\right) \left\{ 1 - \frac{1}{3} \frac{L}{D} \frac{\tan \alpha}{\sin^{\frac{1}{4}}\alpha} \frac{1}{R_L^{\frac{1}{4}}} + \frac{1}{12}\left(\frac{L}{D}\right)^2 \frac{\tan^2\alpha}{\sin^{\frac{1}{2}}\alpha} \frac{1}{R_L^{\frac{1}{2}}} - \cdots \right\}$$

For reasonable Reynolds numbers and high fineness ratios the Magnus force may be approximated by:

$$C_Y = \frac{C_o}{2} \bar{p} \left(\frac{L}{D}\right)^{5/4} \tan \alpha \sin^{3/4}\alpha \, R_L^{-\frac{1}{4}} \qquad \text{(IV.6)}$$

Equation V.6 predicts that all Magnus data should collapse along a line of slope C_o if $\partial C_Y / \partial \bar{p} = C_{Y_{\bar{p}}}$ is plotted against the correlation parameter $\frac{1}{2} \tan \alpha \sin^{3/4}\alpha \left(\frac{L}{D}\right)^{5/4} R_L^{-\frac{1}{4}}$.

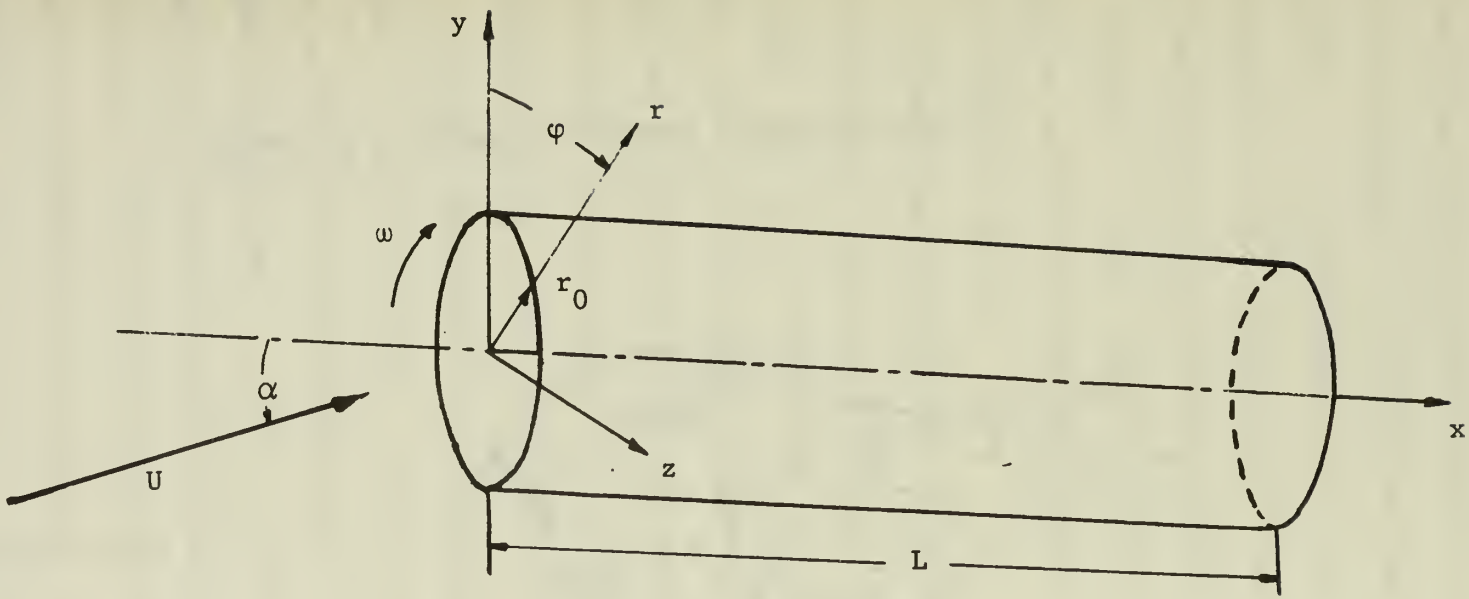

nondimensional spin rate $\bar{p} = \frac{r_o \omega}{U}$

FIGURE IV.1: ROTATING CYLINDER COORDINATE SYSTEM

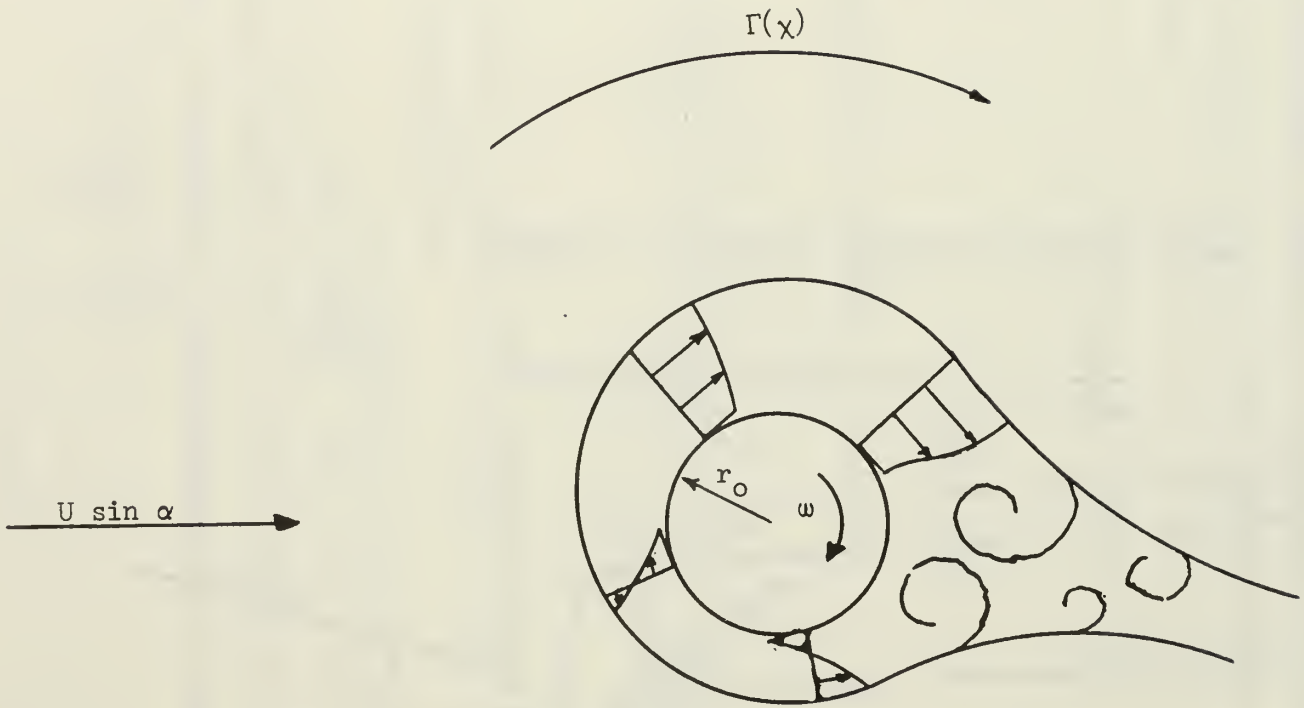

FIGURE IV.2: SPINNING CYLINDER CROSSFLOW ANALOGY

V. EXPERIMENTAL MAGNUS MEASUREMENTS

Theoretical predictions of Magnus side force based upon vorticity shed into the outer flow show nonlinear variation with angle of attack. Experimental Magnus measurements were used to compare actual side force production to that predicted by theory and to establish the values of the empirical factors in equations V.5 and V.6. For this purpose the model configuration selected for study had a tangent-ogive nose followed by a constant 2.95 inch diameter cylindrical afterbody. The afterbody length was varied to provide three missile length-to-diameter ratios, L/D, of 9.9, 7.8 and 6.0.

The model was machined from aluminum and carefully balanced to reduce vibrational loads when spinning. Figure VI-1 shows schematically the model, its support system, the balance, and the air motor drive system. The 1/8 horsepower Standard Pneumatic rotary-vane, bi-directional compressed air motor allowed missle rotational rates as high as 3000 RPM to be tested. An electromagnetic tachometer pickup was used in conjunction with a Monsanto 101B counter to determine model spin rate.

A simple beam balance was used to measure the Magnus side force and center of pressure location. Two four-element strain gage bridge circuits were mounted on the beam flexure such that only sideforce and Magnus moment were measured. Air motor pressure lines were in the vertical plane of the balance to reduce pressurization effects on balance output. A subsequent balance calibration showed that for pressures less than 80 psia the interaction of line pressure and sideforce measurement was negligible. Figure VI.2 shows the wiring diagram for the balance system.

The bridge circuit outputs were amplified and displayed on a HP 7100 B two channel chart recorder. The sting balance system was calibrated by hanging known weights at known distances from the strain gage locations and plotting the applied moment verses chart recorder output. The data reduction program in the Appendix was used to calculate the aerodynamic coefficients. Figure VI-3 shows the model mounted in the wind tunnel.

Data was taken at a constant nominal Reynolds number based on missile length of 1×10^6 and at angles of attack up to 15 degrees. Sideforce production at seven nondimensional spin rates between $\pm$ 0.4 was measured at each angle of attack. Air motor supply pressure was adjusted until the desired spin rate was established. Figure VI-4 through VI-6 show the resulting Magnus force coefficients and the location of the Magnus force center of pressure with respect to the missile base. These figures show a nonlinear variation of sideforce coefficient with angle of attack at constant nondimensional spin rate. The Magnus center of pressure is seen to be approximately one third of the missile length from the base for all the cases tested. Center of pressure location was insensitive to angle of attack and spin rate. The L/D = 9.9 data, however, show movement of the center of pressure with both angle of attack and spin rate for angles of attack less than ten degrees. Sideforce coefficient at constant angle of attack and spin rate is dependent upon missile L/D. Figure VI-7 shows this effect of L/D on the Magnus sideforce coefficient for a non-dimensional spin rate of 0.2.

Theory predicts a linear behavior of sideforce coefficient with nondimensional spin rate $\bar{p}$. Figure VI-8 presents the experimental

data plotted in such a way to test this result. The experimental sideforce coefficients were divided by the nondimensional spin rate to calculate $C_{Y_{\bar{p}}} = \partial C_Y / \partial \bar{p}$. If sideforce coefficient is linear in $\bar{p}$ all the data should collapse to a single line when $C_{Y_{\bar{p}}}$ is plotted against angle of attack. Figure VI-8 shows that for a constant missile L/D the data show an excellent agreement with this theoretical result. Also shown on Figure VI-8 is the linear theory prediction of Kelly[1]. The data show excellent agreement with the linear theory at angle of attack less than five degrees. At angles greater than five degrees the data show nonlinear behavior with angle of attack.

An attempt to correlate the data with equation V-5 was unsuccessful. The data reduction program calculated the value of the correlation constant C_1 for each experimental point. Values of C_1 ranging from zero to three resulted. The value of C_1 increased as missle L/D and angle of attack increased. No single value of C_1 fits the experimental data. Figure VI-9 shows a comparison of equation V-5 with the value of C_1 taken as unity. Equation V-5 consistently overestimates the Magnus coefficient at angles of attack less than approximately ten degrees and underestimates the Magnus force at higher angles.

Figure VI-10 shows the experimental data plotted against the correlation parameter of equation V-6. Excellent agreement with this correlation was found. The data of the higher L.D ratio missle shapes collapsed about a straight line of slope 6.6. The L/D = 6.0 data also collapsed as predicted but at a value of the correlation constant equal to six.

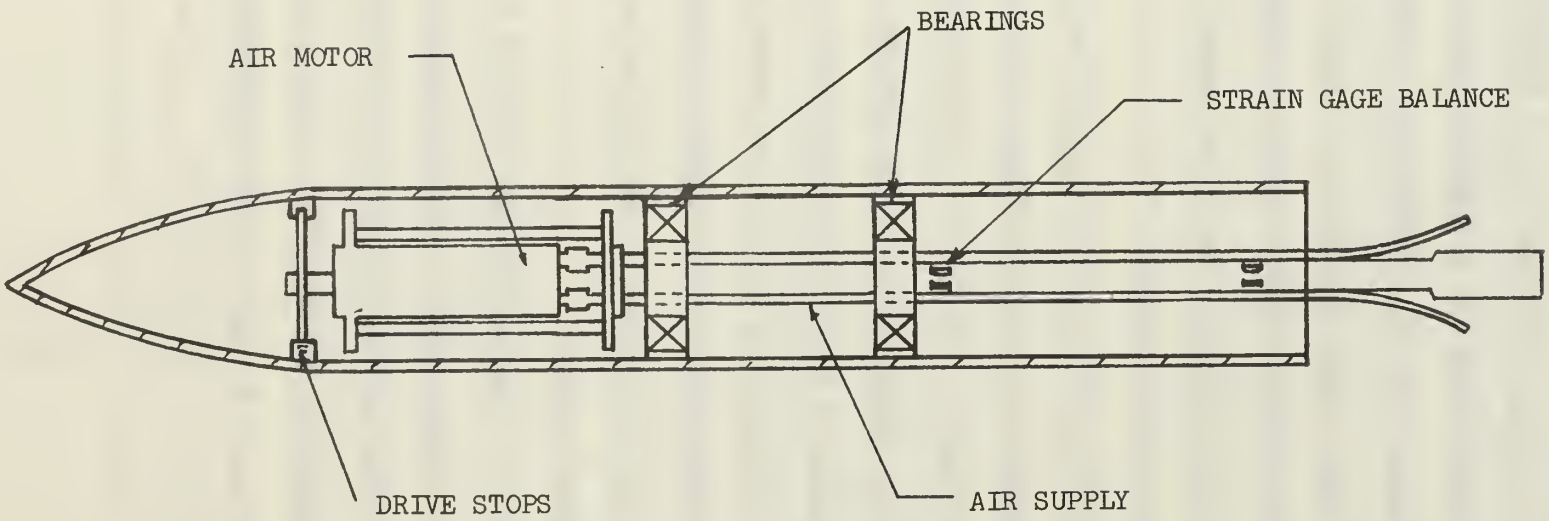

Figure V.1: Details of the Test Model

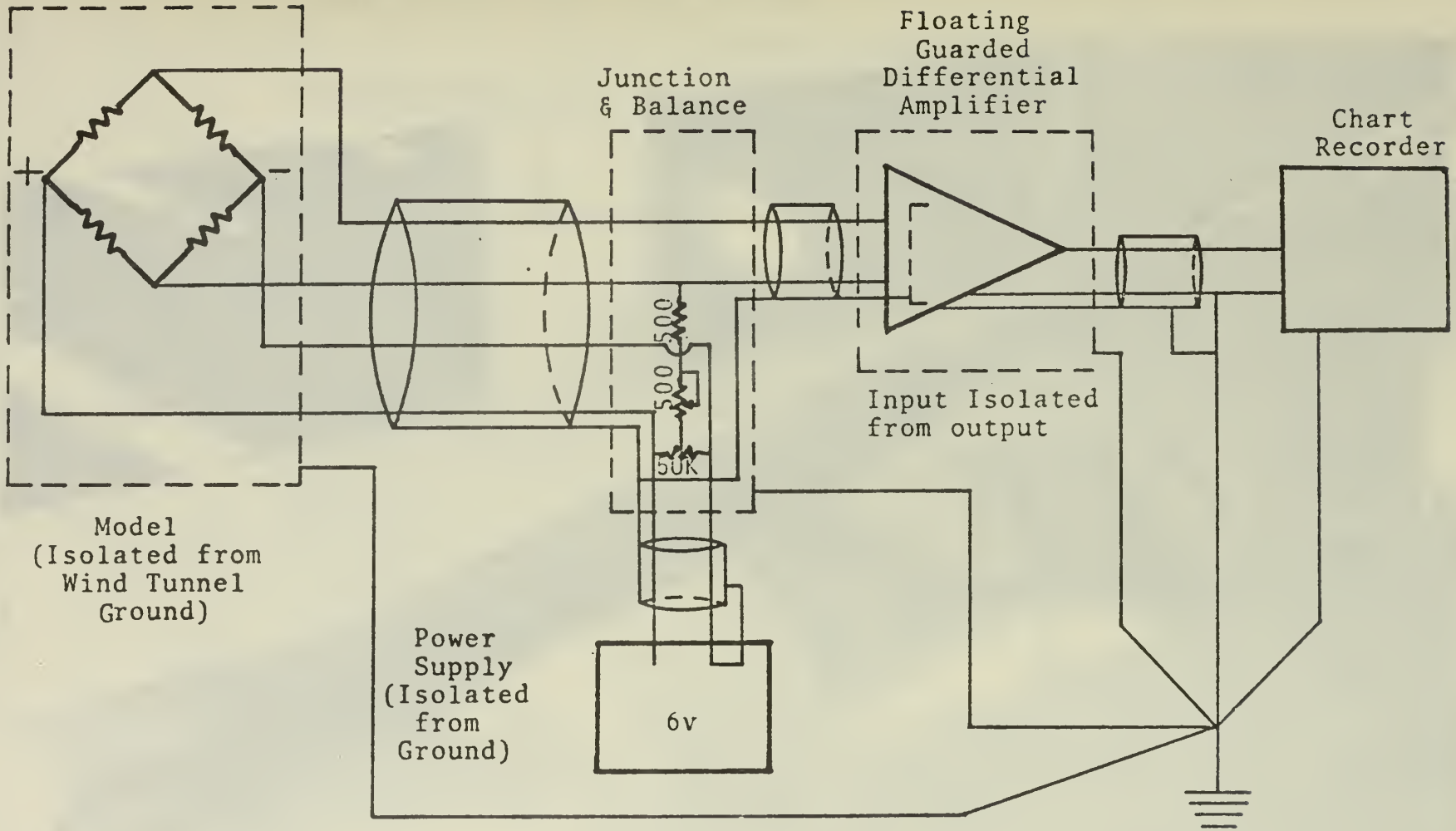

Figure V.2: Wiring Schematic

Figure V.3: L/D = 9.9 Test Model

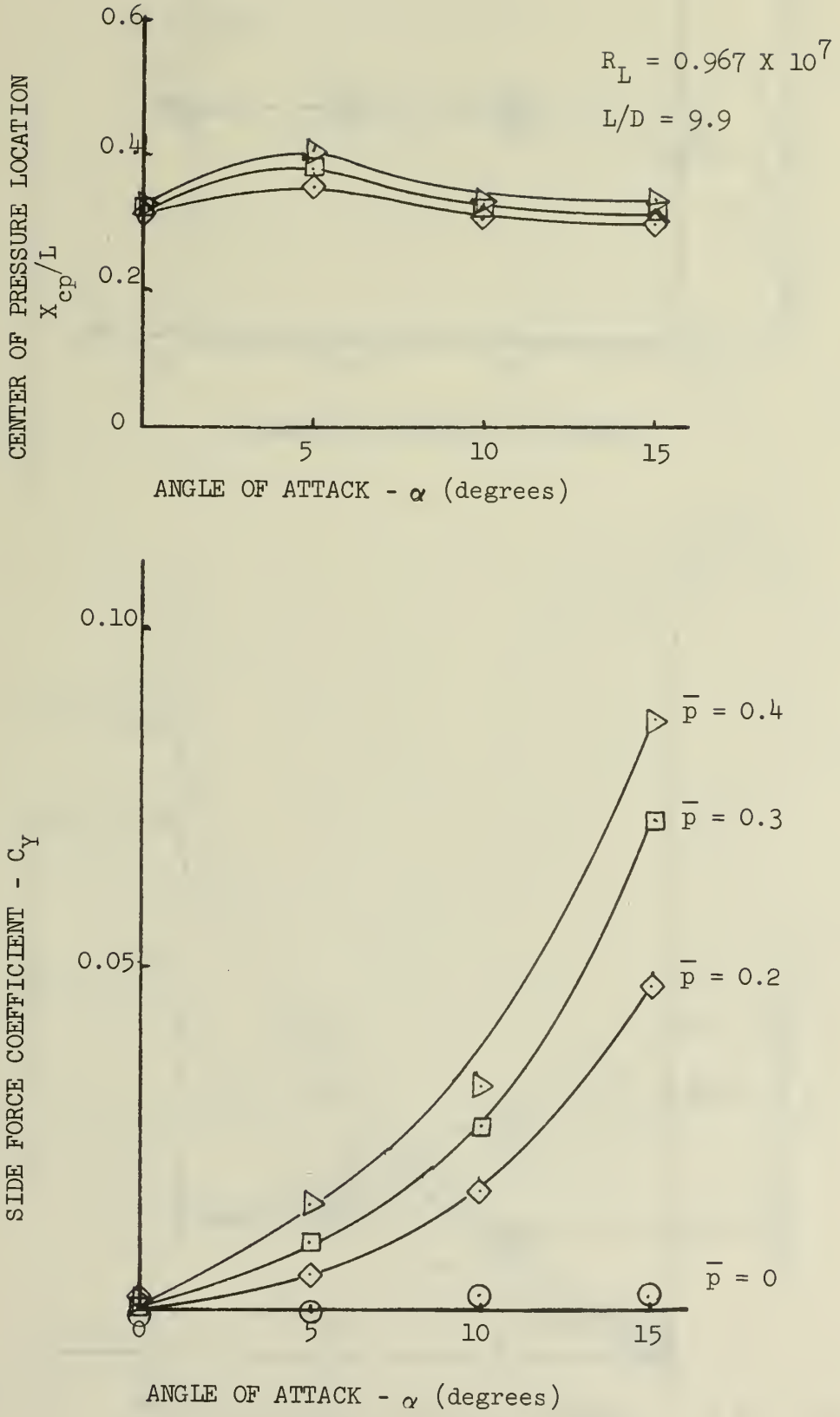

Figure V.4: Magnus Force and Center of Pressure for a 9.9 L/D Spinning Missile

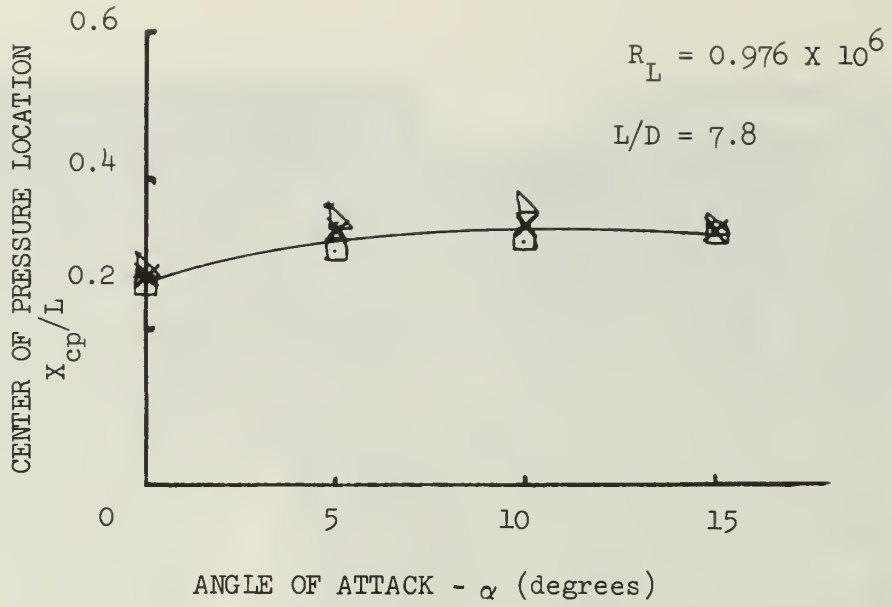

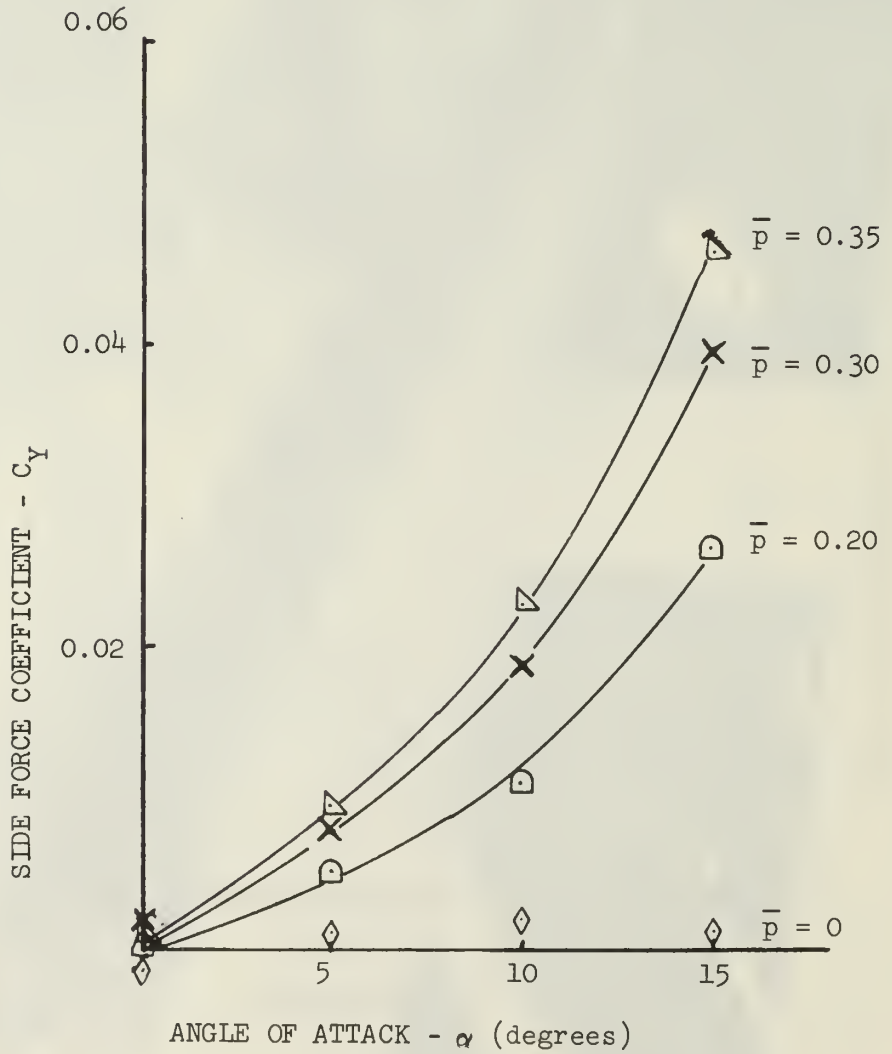

Figure V.5: Magnus Force and Center of Pressure for a 7.8 L/D Spinning Missile

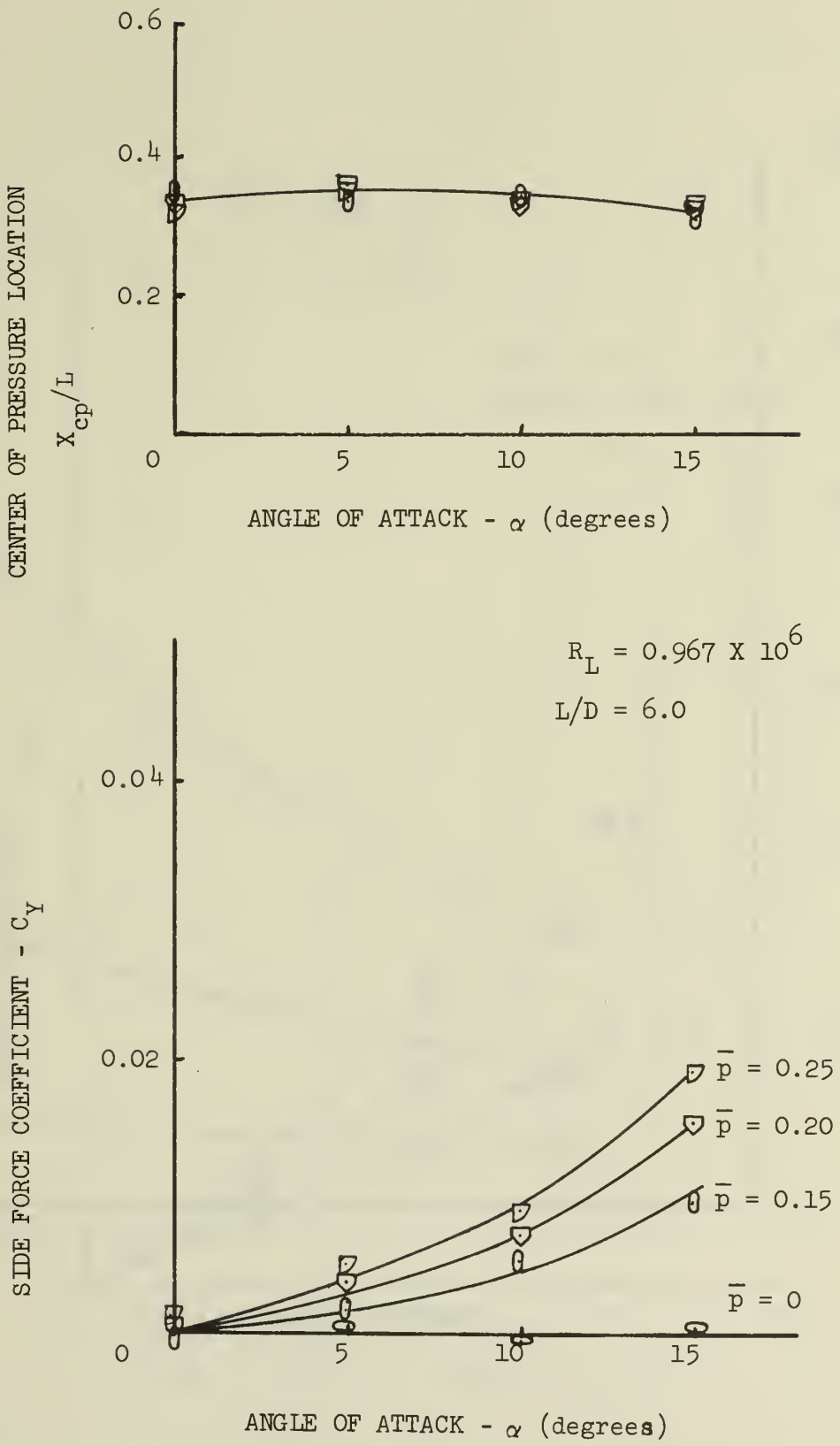

Figure V.6: Magnus Force and Center of Pressure for a 6.0 L/D Spinning Missile

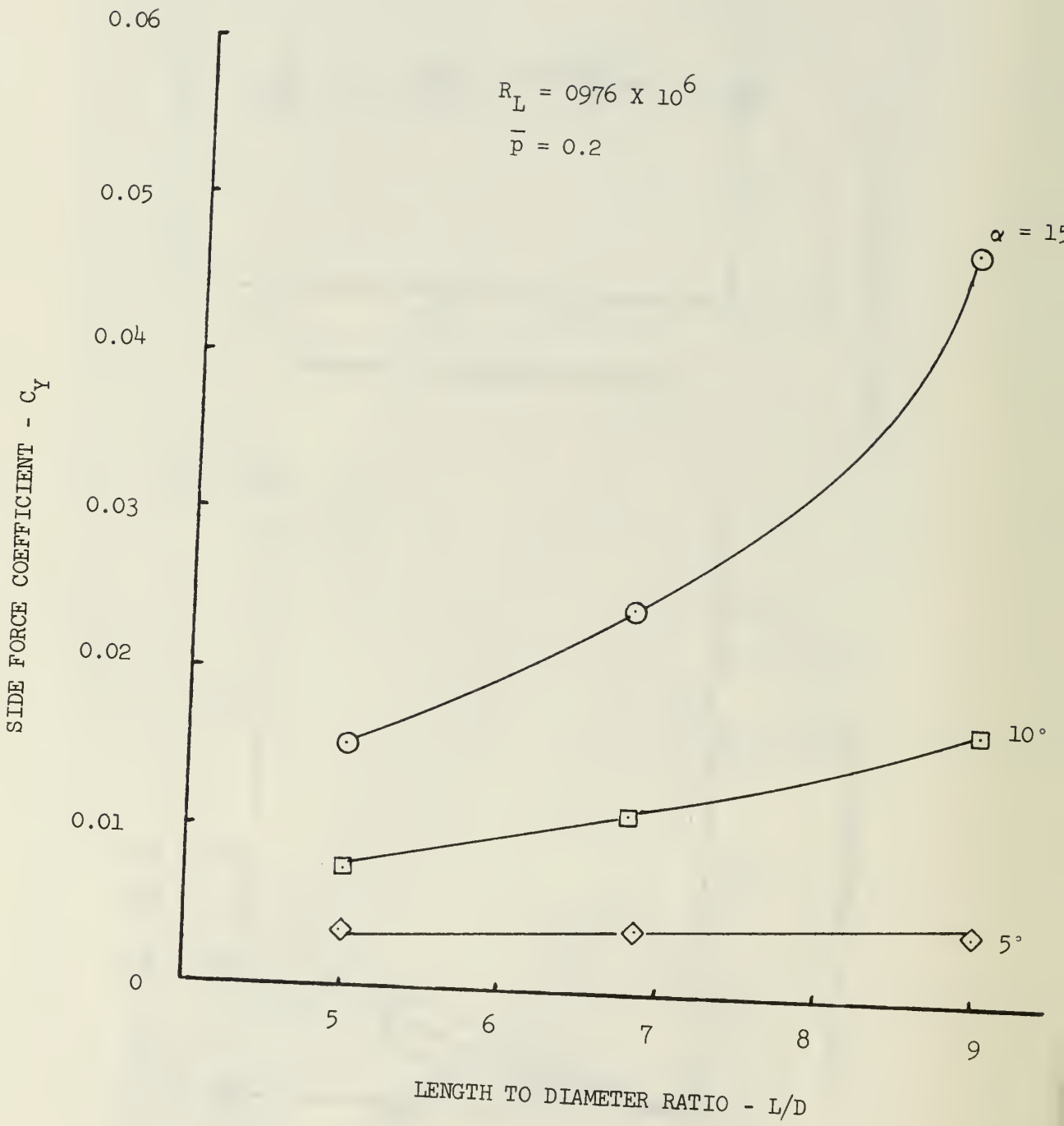

Figure V.7: Magnus Force Variation with L/D at Constant Angle of Attack and Spin Rate

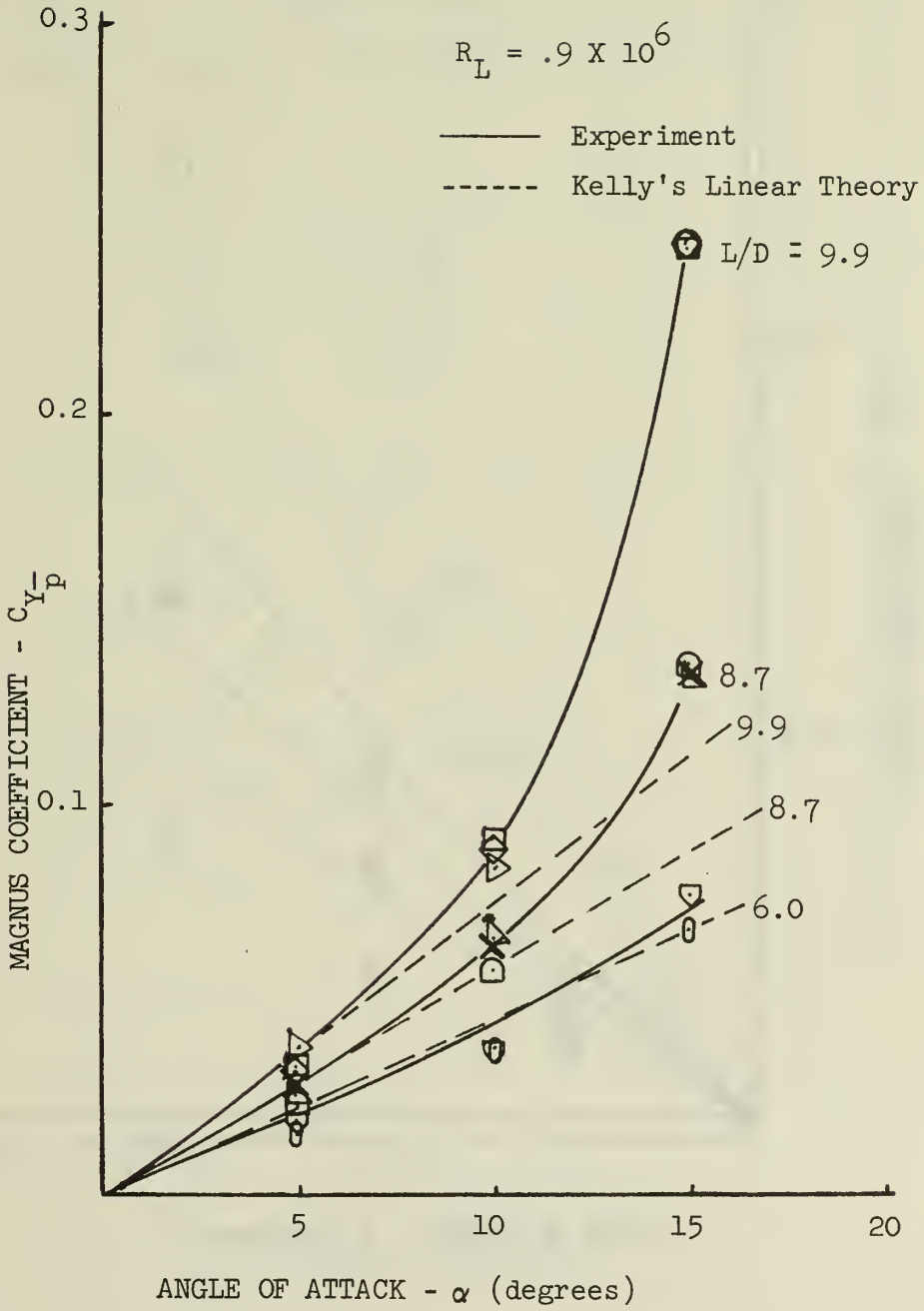

Figure V.8: Magnus Force Coefficient $C_{Y_{\bar{p}}}$

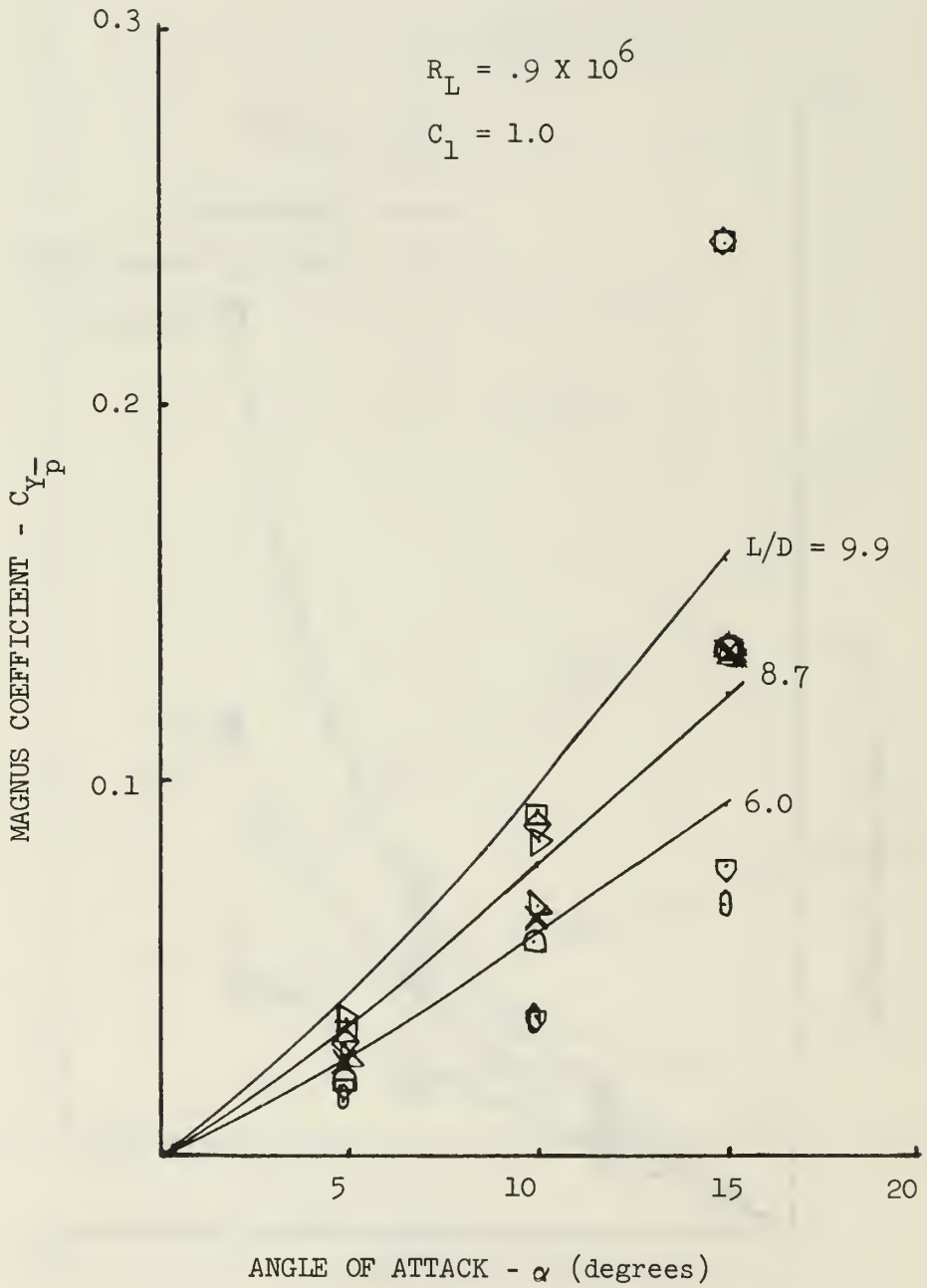

Figure V.9: Magnus Force Comparison with Equation V.5.

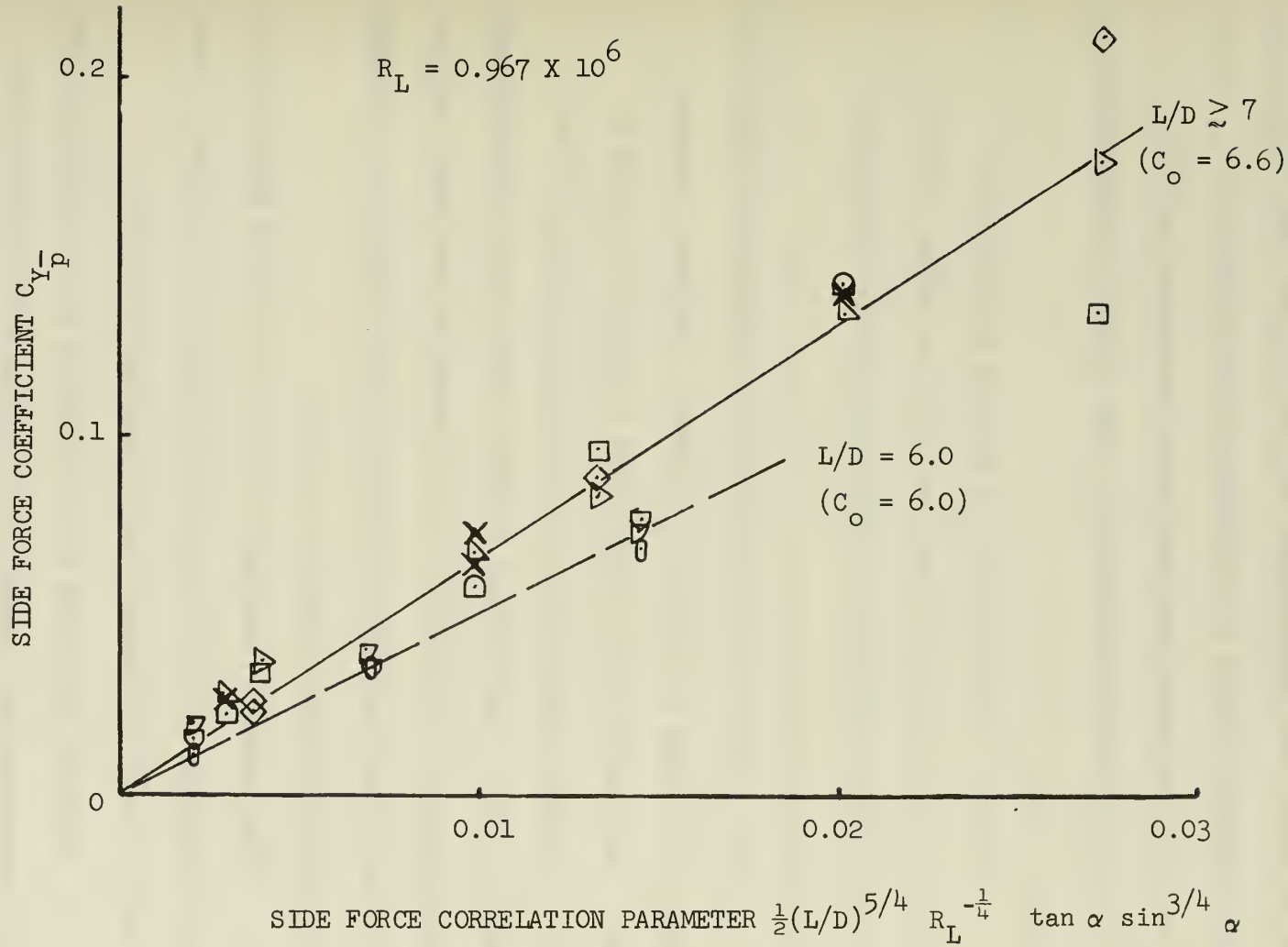

Figure V.10: Magnus Force Correlation

VI. CONCLUSIONS

A comparison of the experimental data in the previous section with theory leads the author to the following conclusions:

1. For the configurations tested the Magnus coefficient is linear in spin rate for constant R_L, α and L/D for nondimensional spin rates less than $\pm$ 0.4.

2. Kelly's linear theory can predict accurately the variation of C_{Y_p} with L/D and R_L only at very low angles of attack (in the case of the configuration tested the angle of attack must be less than five degrees.)

3. The crossflow analogy prediction that Magnus coefficient is nonlinear with angle of attack is accurate. The data, however, only match the theory if the linear term in angle of attack is neglected. It might, therefore, be concluded that although the Magnus effects due to the attached boundary layer growth (displacement and shearing stress contributions) are important at very small angles of attack, the primary mechanism of Magnus force production is through shed vorticity even at small angles of attack.

4. The crossflow analogy leads to an accurate Magnus force correlation parameter if L/D is sufficiently high (in the case of the present data L/D must be greater than approximately seven).

5. Iverson[5] has shown that the Magnus force coefficient for supersonic freestream Mach numbers also show good correlation until the crossflow is near sonic. The correlation constant C_o is expected to be an increasing function of the crossflow Mach number until this velocity is reached. At this point the parameter C_o will remain relatively

constant because of the inability of shed vorticity to reach the outer supersonic flow. The experimental value of C_o for incompressible crossflow Mach numbers has been determined by this study to be 6.6 if the coefficient is based upon side area. The experimental data therefore correlate well with the prediction:

$$C_{Y_p} = 3.3\, R_L^{\frac{1}{4}}\, (L/D)^{5/4} \alpha^{7/4}$$

for angles of attack less than fifteen degrees.

VII. CITED REFERENCES

1. Kelly, H. R. "An Analytical Method for Predicting the Magnus Forces and Moments on Spinning Projectiles" TM-1634, 1954, U.S. Naval Ordnance Test Station, China Lake, California.

2. Power, H. L. "Boundary Layer Contributions to the Magnus Effect on a Spinning Cylinder" PhD thesis, November 1971, Aerospace Engineering Department, Iowa State University, Ames, Iowa.

3. Power, H. L. and J. D. Iverson "Magnus Effect on Spinning Bodies of Revolution" AIAA Journal, Vol. 11, No. 4, April 1973, pp 417-418.

4. Thoman, D. C. and Szewezyk, A. A. "Numerical Solutions of Time Dependent Two-Dimensional Flow of a Viscous, Incompressible Fluid over Stationary and Rotating Cylinder" TR 66-14, July 1966, Dept. of Mechanical Engineering, University of Notre Dame, Notre Dame, Indiana.

5. Iverson, J. D. "Correlation of Magnus Force Data for Slender Spinning Cylinders" AIAA Paper No 72-966, September 1972.

VIII. LIST OF FIGURES

Figure		Page
IV.1:	Rotating Cylinder Coordinate System	9
IV.2:	Spinning Cylinder Crossflow Analogy	10
V.1:	Details of Model, Air Motor and Balance	14
V.2:	Wiring Schematic	15
V.3:	L/D = 9.9 Test Model	16
V.4:	Magnus Force and Center of Pressure Location for a 9.9 L/D Spinning Missile	17
V.5:	Magnus Force and Center of Pressure Location for a 7.8 L/D Spinning Missile	18
V.6:	Magnus Force and Center of Pressure Location for a 6.0 L/D Spinning Missile	19
V.7:	Magnus Force Variation with L/D at Constant Angle of Attack and Spin Rate	20
V.8:	Magnus Force Coefficient C_{Y_p}	21
V.9:	Magnus Force Comparison With Equation V.5	22
V.10:	Magnus Force Correlation	23

COMPUTER PROGRAM FOR DATA REDUCTION

```
      READ (5,100)  B,TCF,RK1,RK2,N
  100 FORMAT (5E10.0)
      READ (5,100) X,D,PA,TF  ,R1L
C     B IS DISTANCE BETWEEN GAGES (IN) ,TCF IS THE TUNNEL CALIBRATION
C     FACTOR (CM H20/PSF),K1 & K2 ARE BALANCE CALIBRATION SLOPES
C     (IN LB/CHART LINES),N IS NUMBER OF DATA POINTS
C     R1L IS DISTANCE FROM FRONT GAGE TO BASE (IN)
C     X IS MISSLE LENGTH (FT),D IS DIAMETER (FT), PA IS ATMOSPHERIC
C     PRESSURE (PSF),TF IS TEST SECTION TEMP.(F)
C     C1 IS SMALL ALPHA CORRELATION CONSTANT AND C2 IS FOR LARGE ALPHA
      DO 1  l=1,N
      READ (5,100) R1,R2,RPM ,A,DP
C     R1 IS FRONT GAGE READING (CHART LINES),R2 IS BACK GAGE READING
C     RPM IS ROTATIONAL SPEED (REV/MIN.),A IS ANGLE OF ATTACK,DP IS
C     DELTA TEST SECTION PRESSURE  (CM H20)
      Y=(RK2*R2-RK1*R1)/B
      XCP=RK1*R1/Y
      XCPR=(XCP+R1L) /(X*12.)
C     Y IS SIDE FORCE (LB), XCP IS CENTER OF PRESSURE LOCATION (IN)
C     XCPR IS NONDIM CP LOCATION FROM BASE
      TR= TF +460.
      RHO= PA*70.73/(1716.*TR)
      ESB= 0.01295*(0.868 +.4*D/X)*D*D*X
      Q=DP*(1.+2.*ESB)/TCF
      V= (2.*Q/RHO)**0.5
C     CY IS SIDE FORCE COEFF BASED ON SIDE AREA
      CY=Y/Q*D*X)
      PHAT=3.1416*D*RPM/(60.*V)
      XMU=(2.26967*TR**1.5)/((TR+198.72)*10.**8.)
      RL=RHO*V*X/XMU
      XLX= X/D
      RAD= A/57.3
      RO= RL*SIN(RAD) /XLX
      XK3=    XLX*(60.97-357.37*XLX/(RL**.5)-227.01*XLX*XLX/RL)/
     1(RL**.5)*3.1416/4.
      SA=SIN(RAD)
      TA=TAN(RAD)
C     CYCP IS THE CORREALATION PARAMETER FOR LARGE ALPHA
      CYCP=XLX**1.25*SA**.75*TA/(2.*RL**.25)
      IF (PHAT) 3,2,3
    2 CYP=0.0
      C1=0.0
      C2=0.0
      GO TO 4
    3 CYP=CY/PHAT
      IF (RAD) 6,5,6
    6 IF (SA) 7,5,7
    7 IF (TA) 8,5,8
    5 C1=0.0
      C2=0.0
```

```
      GO TO 4
    8 C1=4.*RL**.25*(CY/PHAT-XK3*RAD)/(3.1416*XLX**1.25*RAD**1.75)
      C2=2.*CY8RL**.25/(PHAT*SA**.75*TA*XLX**1.25)
    4 WRITE (6,110)
  110 FORMAT (IH,// 19X,'ALPHA',16X,'PHAT',19X,'CY',17X,'XCPR',18X,
     1'CYP',17X,'CYCP' )
      WRITE (6,111) A,PHAT,CY,XCPR,CYP,CYCP
  111 FORMAT  ( 9X,6E20.7)
      WRITE (6,112)
  112 FORMAT (IH,/ 39X,'L/D',18X,'RL',18X,'RC',17X,'C1',18X,'C2')
      WRITE (6,113)  XLX,RL,RC,C1,C2
  113 FORMAT (29X,5E20.7)
    1 CONTINUE
      STOP
      END
```

Distribution List

		No. of Copies
1.	Library Code 0212 Naval Postgraduate School Monterey, CA 93940	2
2.	Department of Aeronautics Code 57 Naval Postgraduate School Monterey, CA 93940	
	Prof. R. W. Bell, Chairman	1
	Prof. H. L. Power	2
	Prof. A. E. Fuhs	1
	Prof. D. J. Collins	1
	Prof. T. H. Gawain	1
	Prof. C. H. Kahr	1
	Prof. L. V. Schmidt	1
3.	Prof. R. R. Fossum Code 023 Dean of Research Administration Naval Postgraduate School Monterey, CA 93940	1
4.	Defense Documentation Center Cameron Station Alexandria, VA 22314	2
5.	Chief of Naval Research Arlington, Virginia 22217	2